Missing traffic data imputation and pattern discovery with a Bayesian augmented tensor factorization model

Xinyu Chen[a], Zhaocheng He[a,*], Yixian Chen[a], Yuhuan Lu[a], Jiawei Wang[a,b]

[a]*Guangdong Provincial Key Laboratory of Intelligent Transportation Systems, Research Center of Intelligent Transportation System, Sun Yat-Sen University, Guangzhou, Guangdong 510006, China*
[b]*Peng Cheng Laboratory (Shenzhen Cyberspace Laboratory), Shenzhen, Guangdong 518000, China*

Abstract

Spatiotemporal traffic data, which represent multidimensional time series on considering different spatial locations, are ubiquitous in real-world transportation systems. However, the inevitable missing data problem makes data-driven intelligent transportation systems suffer from the incorrect response. Therefore, imputing missing values is of great importance but challenging as it is not easy to capture spatiotemporal traffic patterns, including explicit and latent features. In this study, we propose an augmented tensor factorization model by incorporating generic forms of domain knowledge. Specifically, we present a fully Bayesian framework for automatically learning parameters of this model using variational Bayes (VB). Relying on the publicly available urban traffic speed data set collected in Guangzhou, China, experiments on two types of missing data scenarios (i.e., random and non-random) demonstrate that the proposed Bayesian augmented tensor factorization (BATF) model achieves best imputation accuracies and outperforms the state-of-the-art baselines (e.g., Bayesian tensor factorization models). Besides, we discover interpretable patterns from the experimentally learned global parameter, biases, and latent factors that indeed conform to the dynamic of traffic states.

Keywords: Missing data imputation, Pattern discovery, Spatiotemporal traffic data, Bayesian tensor factorization, Variational Bayes

1. Introduction

Missing data problem is common and inevitable in the data-driven intelligent transportation systems, which also exists in several applications (e.g., traffic states monitoring). Although we have many advanced sensors to enable us to collect all of the data as we want, unfortunately, it may be still impossible to avoid data incompleteness because some types of data are sparse by nature. Other types of urban traffic data may be restricted by the spatial coverage of sensors. The uncertainty like communication malfunctions and transmission distortions of sensors when collecting spatiotemporal is another influential factor. Thus, in these contexts, making accurate imputation and improving data quality are critical for supporting the success of any application which makes use of that type of data.

The main idea of missing traffic data imputation can be generally summarized as follows. If we have partially observed data with both spatial and temporal resolution, then a model is required to be capable of discovering spatiotemporal patterns. From a technical perspective, this is similar to the idea of collaborative filtering (Salakhutdinov and Mnih, 2008; Xiong et al., 2010). For example, given a spatiotemporal traffic states matrix (road segment × time series), in order to impute missing values for each single time series (corresponding to each road segment), we can borrow collaborative information from similar road segments (Laa et al., 2018).

To this end, there is a family of matrix factorization techniques, which has been applied to impute missing traffic data in the previous studies (Qu et al., 2008, 2009; Li et al., 2013). Qu et al. (2009) proposed a probabilistic principal component analysis (PPCA) based imputation method for traffic volume data completion, and in their experiments, this method was illustrated to make use of patterns including not only statistical information of traffic flow, but periodicity and local predictability. Within this work, BPCA evaluated by Qu et al. (2008) was proven to be inferior to PPCA. Following this work, Li et al. (2013) demonstrated that using spatial and temporal dependencies could help reduce estimation errors significantly for PPCA based methods. Notably, in these methods, the assumption of strictly daily similarity is not required.

Recently, Rodrigues et al. (2018) applied the multi-output Gaussian processes (GPs) to model the complex spatial and temporal patterns about incomplete traffic speed data. Since the model is capable of considering observation uncertainty and spatial dependencies between nearby road segments, their experiments showed

---

*Corresponding author.
Email addresses: `chenxy346@mail2.sysu.edu.cn` (Xinyu Chen), `hezhch@mail.sysu.edu.cn` (Zhaocheng He), `chenyx96@mail2.sysu.edu.cn` (Yixian Chen), `luyh6@mail2.sysu.edu.cn` (Yuhuan Lu), `wangjw33@mail2.sysu.edu.cn` (Jiawei Wang)
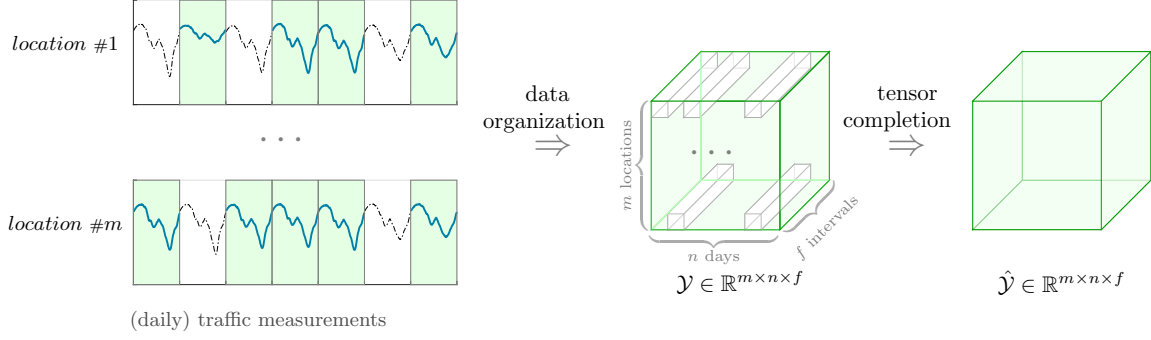
Figure 1: Graphical illustration of the tensor completion task for partially observed traffic measurements.

that the model achieves significantly better results than some state-of-the-art imputation methods including independent GP, PPCA, and Bi-LSTM.

Another choice for modeling spatiotemporal traffic data is through organizing these data into tensors. In the existing studies, tensor completion models for imputing missing traffic data can be summarized into two categories. The first is low-rank tensor completion models which include SiLRTC, FaLRTC, and HaLRTC proposed by Liu et al. (2013), then, the experiments about traffic volume data imputation have indicated that HaLRTC supports the use of spatial information from neighboring locations (Ran et al., 2016). However, these models are sensitive to the observation noises and suffer from the sparsity issue. When dealing with an extremely sparse tensor, they are inferior to capture the global information of the tensor (Zhao et al., 2015a), thus, the imputation accuracy of these models is rather limited.

The second is tensor decomposition for an incomplete tensor, Tan et al. (2013a,b); Asif et al. (2016) employed multilinear tensor decomposition as to estimate missing traffic data, and the extensive experiments demonstrated that the tensor decomposition models outperform the PCA based methods. Performing fully Bayesian treatment on tensor decomposition makes it possible to tackle the non-convex optimization problem underlying tensor decomposition (Xiong et al., 2010; Rai et al., 2014; Zhao et al., 2015a,b) and alleviate the data sparsity issue.

This paper provides a generic solution to multidimensional traffic data modeling using tensor factorization models. Specifically, inspired by Koren et al. (2009); Chen et al. (2018), one aim of this work is to develop an augmented tensor factorization that combines both explicit patterns and latent factors. In a variational Bayes (VB) framework, the model parameters formulated in the augmented tensor factorization are expected to learn by inferring their variational posteriors. In terms of Bayesian tensor factorization, Hu et al. (2015); Rai et al. (2015) also reported that deterministic inference methods such as VB and Expectation Maximization (EM) are more efficient than the close-formed Markov chain Monte Carlo (MCMC).

In this new approach to missing data imputation, we wish to further investigate the semantic interpretability of the augmented tensor factorization, in which we incorporate generic forms of domain knowledge from transportation systems. On considering the missing data scenario and by comparing to the Bayesian tensor factorization models, we finally intend to explore the advantages of newly formulated augmented tensor factorization with fully Bayesian treatment.

2. Preliminaries

A natural way of modeling multidimensional traffic data is in the form of a tensor. In this work, our task is: given a partially observed tensor $\mathcal{Y}$, relying on its algebraic structure, learn from partial elements and further estimate the unobserved elements in this tensor (see Fig. 1). Formally, we use $\mathcal{Y}_\Omega$ to denote the partially observed elements in $\mathcal{Y}$, and where Ω is the set of observation index. For simplicity of notation, we only investigate the tensor factorization for third-order tensor $\mathcal{Y} \in \mathbb{R}^{m \times n \times f}$ in this study. And we further define $\mathcal{O} \in \mathbb{R}^{m \times n \times f}$ to be a binary tensor with such that $o_{ijt} = 1$ if y_{ijt} is observed (i.e., $(i, j, t) \in \Omega$), and $o_{ijt} = 0$ otherwise.

Regarding such formulated tensor completion task, we summarize the main developed tensor models as follows:

(a) *Basic tensor factorization*. To identify an underlying low-dimensional representation of r latent factors, one well-established model is CANDECOMP/PARAFAC(CP) decomposition and we can factorize $\mathcal{Y}$ into factor matrices $U \in \mathbb{R}^{m \times r}$, $V \in \mathbb{R}^{n \times r}$ and $X \in \mathbb{R}^{f \times r}$ (Kolda and Bader, 2009). For any (i, j, t)-th element of the tensor $\mathcal{Y}$, there exists an approximation which is a multilinear combination of r latent factors from each factor matrix as

$$y_{ijt} \approx \sum_{k=1}^{r} u_{ik} v_{jk} x_{tk}, \forall (i, j, t). \tag{1}$$

(b) *Low-rank tensor completion*. By introducing trace norm to fill in tensors' missing elements, Liu et al. (2013) developed a sequence of low-rank tensor completion algorithms by converting the nonconvex rank minimization

problem to a convex optimization (i.e., trace norm optimization) problem. In their definition, the optimization formula is

$$\min_{\mathcal{X}} : \sum_{i=1}^{3} \alpha_i \|\mathcal{X}_{(i)}\|_*$$
$$\text{s.t.} : \mathcal{X}_\Omega = \mathcal{Y}_\Omega, \tag{2}$$

where α_is are constants satisfying $\alpha_i \geq 0$ and $\sum_{i=1}^{3} \alpha_i = 1$. In the objective function, $\mathcal{X}_{(i)}$ denotes the matrix unfolded along i-th mode and $\|\mathcal{X}_{(i)}\|_*$ represents the trace norm of $\mathcal{X}_{(i)}$.

(c) *Bayesian tensor factorization.* The goal of tensor factorization is to find a low-rank approximation, thus, taking CP factorization as an example, we can in effect minimize the loss function to achieve a tensor factorization by

$$\mathcal{J} = \sum_{(i,j,t) \in \Omega} (y_{ijt} - \sum_{k=1}^{r} u_{ik} v_{jk} x_{tk})^2 + w_u \mathcal{R}_u + w_v \mathcal{R}_v + w_x \mathcal{R}_x, \tag{3}$$

where $\mathcal{R}_u, \mathcal{R}_v, \mathcal{R}_x$ are regularization terms related to the factor matrices U, V, X respectively, and their weights are $\{w_u, w_v, w_x\}$. Unfortunately, one common thing associated with this optimization is the non-convex problem, thus leading to the development of Bayesian Gaussian tensor factorization approaches (Xiong et al., 2010; Rai et al., 2014; Hu et al., 2015; Rai et al., 2015; Zhao et al., 2015a,b).

In terms of experimental evaluation, spatiotemporal traffic data sets collected from transportation systems can be easily represented by a multidimensional array (i.e., tensor). Fig. 1 illustrates the framework for imputing the missing values of spatiotemporal traffic data.

3. Bayesian augmented tensor factorization model

In the following, we first introduce the mathematical formula of the proposed augmented tensor factorization. Subsequently, we briefly discuss the Bayesian treatment for solving this factorization model. Finally, we infer the variational posterior of parameters and hyper-parameters in the Bayesian graphical network and derive an implementation for the augmented tensor factorization using VB.

3.1. Augmented tensor factorization

Typically, CP decomposition maps multidimensional data to a joint latent factor space of dimensionality r, such that complicated interactions are modeled as inner products in that space (see Eq. (1)). In this work, we build a semantic combination of explicit patterns and latent factors on the tensor model and propose an augmented tensor factorization with the following formula, i.e.,

$$y_{ijt} \approx \mu + \phi_i + \theta_j + \eta_t + \sum_{k=1}^{r} u_{ik} v_{jk} x_{tk}, \forall (i,j,t), \tag{4}$$

where $\mu \in \mathbb{R}$ is a global parameter responsible for all tensor elements, $\boldsymbol{\phi} \in \mathbb{R}^m, \boldsymbol{\theta} \in \mathbb{R}^n, \boldsymbol{\eta} \in \mathbb{R}^f$ are bias vectors relative to each dimension, and $U \in \mathbb{R}^{m \times r}, V \in \mathbb{R}^{n \times r}, X \in \mathbb{R}^{f \times r}$ are factor matrices controlling the interactions among different dimensions. In this model, global parameter μ and bias vectors $\{\boldsymbol{\phi}, \boldsymbol{\theta}, \boldsymbol{\eta}\}$ indicate the explicit patterns, while factor matrices $\{U, V, X\}$ indicate the latent factors. Fig. 2 presents a concise graph of the proposed tensor model.

In the proposed model, parameter μ serves as a global parameter for approaching the overall average of tensor elements. Based on μ, bias along each dimension captures the explicit patterns or features (Koren et al., 2009). In the transportation field, it is also valuable to model the bias of spatial and temporal attributes (Chen et al., 2018). Now, for example, consider the case that the average time series speed of collected road segments is 39 km/h. Further, suppose that one selected road segment tends to be 10 km/h higher than the average, and the specific time period tends to be 5 km/h lower than the average. Then, the speed value for the selected road segment at that time period would be roughly approximated by 44 km/h (i.e., $39 + 10 - 5 = 44$).

3.2. Bayesian framework

We propose to use Bayesian inference methods to learn the parameters $\{\mu, \boldsymbol{\phi}, \boldsymbol{\theta}, \boldsymbol{\eta}, U, V, X\}$ from the data tensor $\mathcal{Y}$. Since Gaussian assumption over tensor factorization has an equivalent form to the common-used loss function (Xiong et al., 2010), therefore, we assume that each element of $\mathcal{Y}$ follows independent Gaussian distribution, i.e.,

$$y_{ijt} \sim \mathcal{N}(\mu + \phi_i + \theta_j + \eta_t + \sum_{k=1}^{r} u_{ik} v_{jk} x_{tk}, \tau^{-1}), \forall (i,j,t), \tag{5}$$
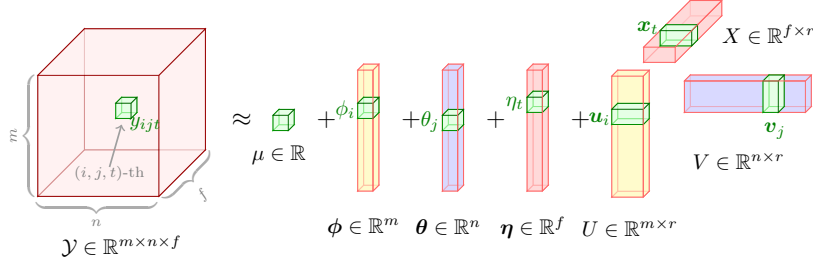
Figure 2: Proposed augmented tensor factorization to tensor completion.

where the notation $\mathcal{N}(\cdot)$ denotes Gaussian distribution, and τ is the precision (inverse of the variance) which is a universal parameter for all tensor elements. From a probability perspective, Eq. (5) is capable of modeling the data uncertainty and randomness of $\mathcal{Y}$.

The basic idea of Bayesian inference is to derive the posterior distribution as a consequence of prior distribution and likelihood function in a Bayesian setting. To learn the model parameters in Eq. (5), we need to place conjugate priors on model parameters, i.e.,

$$
\begin{aligned}
\mu, \phi_i, \theta_j, \eta_t &\sim \mathcal{N}(\mu_0, \tau_0^{-1}), \forall (i,j,t), \\
\boldsymbol{u}_i &\sim \mathcal{N}(\boldsymbol{\mu}_u, \Lambda_u^{-1}), \forall i, \\
\boldsymbol{v}_j &\sim \mathcal{N}(\boldsymbol{\mu}_v, \Lambda_v^{-1}), \forall j, \\
\boldsymbol{x}_t &\sim \mathcal{N}(\boldsymbol{\mu}_x, \Lambda_x^{-1}), \forall t, \\
\tau &\sim \mathrm{Gamma}(a_0, b_0),
\end{aligned}
\tag{6}
$$

where the vector $\boldsymbol{u}_i \in \mathbb{R}^r$ is the i-th row of factor matrix $U \in \mathbb{R}^{m \times r}$ with dimensionality r, the vector $\boldsymbol{v}_j \in \mathbb{R}^r$ is the j-th row of factor matrix $V \in \mathbb{R}^{n \times r}$, and the vector $\boldsymbol{x}_t \in \mathbb{R}^r$ is the t-th row of factor matrix $X \in \mathbb{R}^{f \times r}$. The probability density function (PDF) of the Gamma distribution (i.e., $\mathrm{Gamma}(\cdot)$) with shape a and rate b is

$$
\mathrm{Gamma}(\tau \mid a, b) = \frac{1}{\Gamma(a)} b^a \tau^{a-1} \exp(-b\tau),
\tag{7}
$$

where the notation $\Gamma(\cdot)$ denotes Gamma function.

Referring to the Bayesian probabilistic matrix factorization proposed by Salakhutdinov and Mnih (2008), we further place Gaussian-Wishart priors on hyperparameters $\{\boldsymbol{\mu}_u, \Lambda_u, \boldsymbol{\mu}_v, \Lambda_v, \boldsymbol{\mu}_x, \Lambda_x\}$ as follows

$$
\begin{aligned}
\boldsymbol{\mu}_u, \Lambda_u &\sim \mathcal{N}(\boldsymbol{\mu}_u \mid \boldsymbol{\mu}_0, (\beta_0 \Lambda_u)^{-1}) \times \mathcal{W}(\Lambda_u \mid W_0, \nu_0), \\
\boldsymbol{\mu}_v, \Lambda_v &\sim \mathcal{N}(\boldsymbol{\mu}_v \mid \boldsymbol{\mu}_0, (\beta_0 \Lambda_v)^{-1}) \times \mathcal{W}(\Lambda_v \mid W_0, \nu_0), \\
\boldsymbol{\mu}_x, \Lambda_x &\sim \mathcal{N}(\boldsymbol{\mu}_x \mid \boldsymbol{\mu}_0, (\beta_0 \Lambda_x)^{-1}) \times \mathcal{W}(\Lambda_x \mid W_0, \nu_0),
\end{aligned}
\tag{8}
$$

where the marginal distribution over $\{\Lambda_u, \Lambda_v, \Lambda_x\}$ is a Wishart distribution (i.e., $\mathcal{W}(\cdot)$), and the conditional distribution over $\{\boldsymbol{\mu}_u, \boldsymbol{\mu}_v, \boldsymbol{\mu}_x\}$ given $\{\Lambda_u, \Lambda_v, \Lambda_x\}$ is a multivariate Gaussian distribution. Specifically, the PDF of Wishart distribution is given by

$$
\mathcal{W}(\Lambda \mid W, \nu) = \frac{1}{C} |\Lambda|^{\frac{1}{2}(\nu - r - 1)} \exp\left(-\frac{1}{2}\mathrm{tr}(W^{-1}\Lambda)\right),
\tag{9}
$$

where C is a normalization constant, and the notation $\mathrm{tr}(\cdot)$ denotes the trace of a squared matrix. Λ follows Wishart distribution with ν degrees of freedom and a $r \times r$ scale matrix W.

For graphical model of the proposed Bayesian augmented tensor factorization (BATF), see Fig. 3. In the following, we use Θ to represent $\{\mu, \phi, \boldsymbol{\theta}, \boldsymbol{\eta}, U, V, X, \tau, \boldsymbol{\mu}_u, \Lambda_u, \boldsymbol{\mu}_v, \Lambda_v, \boldsymbol{\mu}_x, \Lambda_x\}$ for reducing the verbosity. In terms of Eq. (4), the aim is to derive the model parameters $\{\mu, \phi, \boldsymbol{\theta}, \boldsymbol{\eta}, U, V, X\}$.

3.3. Posterior inference using VB

Bayesian tensor factorization models have attracted much interest in collaborative filtering (Xiong et al., 2010), image completion (Zhao et al., 2015a,b), and relational graph analysis (Schein et al., 2016) (e.g., social network and international relation). In this part, we describe the VB inference for the proposed BATF.

3.3.1. Fundamentals of VB

VB is a deterministic inference method for approximating posterior distributions. In this study, we wish to seek a distribution $q(\Theta)$ to approximate the true posterior distribution $p(\Theta \mid \mathcal{Y}_\Omega)$ by minimizing the Kullback-Leibler (KL) divergence. The KL divergence is defined as follows
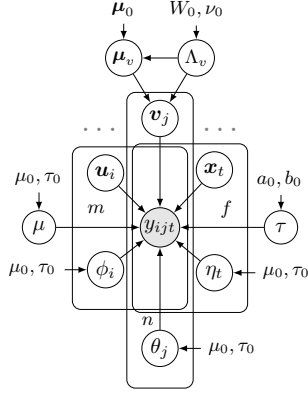
4

Figure 3: Graphical model of the BATF. The observations $y_{jit}, (i, j, t) \in \Omega$ is shown by the shaded node, while the intersection of three plates illustrates that the third-order tensor is partially observed.

$$
\begin{aligned}
\mathrm{KL}(q(\Theta) \parallel p(\Theta \mid \mathcal{Y}_\Omega)) &= \int q(\Theta) \ln \frac{q(\Theta)}{p(\Theta \mid \mathcal{Y}_\Omega)} d\Theta \\
&= \ln p(\mathcal{Y}_\Omega) - \int q(\Theta) \ln \frac{p(\mathcal{Y}_\Omega, \Theta)}{q(\Theta)} d\Theta,
\end{aligned}
\tag{10}
$$

where $\ln p(\mathcal{Y}_\Omega)$ represents the model evidence which is a constant, and its lower bound is defined as

$$
\mathcal{L}(q) = \int q(\Theta) \ln \frac{p(\mathcal{Y}_\Omega, \Theta)}{q(\Theta)} d\Theta.
$$

According to the mean-field approximation, the variational posterior distribution $q(\Theta)$ is fully factorized by

$$
\begin{aligned}
q(\Theta) =& q(\mu) \times \prod_{i=1}^{m} q(\phi_i) q(\boldsymbol{u}_i) \times \prod_{j=1}^{n} q(\theta_j) q(\boldsymbol{v}_j) \times \prod_{t=1}^{f} q(\eta_t) q(\boldsymbol{x}_t) \\
& \times q(\tau) \times q(\boldsymbol{\mu}_u, \Lambda_u) \times q(\boldsymbol{\mu}_v, \Lambda_v) \times q(\boldsymbol{\mu}_x, \Lambda_x).
\end{aligned}
\tag{11}
$$

For any s-th variable Θ_s, the equivalent form for maximizing the lower bound $\mathcal{L}(q)$ is given as follows

$$
\ln q(\Theta_s) = \mathbb{E}_{q(\Theta \setminus \Theta_s)} [\ln p(\mathcal{Y}_\Omega, \Theta)] + \mathrm{const},
\tag{12}
$$

where the notation $\mathbb{E}_{q(\Theta \setminus \Theta_s)} [\cdot]$ denotes an expectation with respect to the distributions $q(\Theta \setminus \Theta_s)$ over all variables except Θ_s. Putting Eqs. (5), (6) and (8) together, the joint distribution $p(\mathcal{Y}_\Omega, \Theta)$ mentioned in Eq. (12) is

$$
\begin{aligned}
p(\mathcal{Y}_\Omega, \Theta) =& p(\mathcal{Y}_\Omega \mid \mu, \boldsymbol{\phi}, \boldsymbol{\theta}, \boldsymbol{\eta}, U, V, X, \tau) \times p(\mu) \times \prod_{i=1}^{m} p(\phi_i) p(\boldsymbol{u}_i \mid \boldsymbol{\mu}_u, \Lambda_u) \\
& \times \prod_{j=1}^{n} p(\theta_j) p(\boldsymbol{v}_j \mid \boldsymbol{\mu}_v, \Lambda_v) \times \prod_{t=1}^{f} p(\eta_t) p(\boldsymbol{x}_t \mid \boldsymbol{\mu}_x, \Lambda_x) \times p(\tau) \\
& \times p(\boldsymbol{\mu}_u, \Lambda_u) \times p(\boldsymbol{\mu}_v, \Lambda_v) \times p(\boldsymbol{\mu}_x, \Lambda_x).
\end{aligned}
\tag{13}
$$

3.3.2. The variational posterior distribution of μ

Starting with variational posterior distribution $q(\mu)$ with respect to the model parameter μ and applying Eqs. (12) and (13), we get the logarithm form of $q(\mu)$ as

$$
\begin{aligned}
\ln q(\mu) &= \mathbb{E}_{q(\Theta \setminus \mu)}[\ln p(\mathcal{Y}_\Omega, \Theta)] + \mathrm{const} \\
&= -\sum_{(i,j,t) \in \Omega} \frac{1}{2} \mathbb{E}[\tau(z_{ijt} - \mu)^2] - \frac{1}{2} \tau_0 \mathbb{E}[(\mu - \mu_0)^2] + \mathrm{const} \\
&= -\frac{1}{2} (\mathbb{E}[\tau] \sum_{(i,j,t) \in \Omega} o_{ijt} + \tau_0) \mu^2 + (\mathbb{E}[\tau] \sum_{(i,j,t) \in \Omega} \mathbb{E}[z_{ijt}] + \tau_0 \mu_0) \mu + \mathrm{const},
\end{aligned}
\tag{14}
$$

where the notation $\mathbb{E}_{q(\Theta \setminus \mu)} [\cdot]$ denotes an expectation with respect to the distributions $q(\Theta \setminus \mu)$ over all variables except μ. Equivalently, the variational posterior introduced in Eq. (14) is $q(\mu) = \mathcal{N}(\tilde{\mu}, \tilde{\tau}^{-1})$ with such that

$$\tilde{\mu} = \tilde{\tau}^{-1}(\mathbb{E}\left[\tau\right] \sum_{(i,j,t)\in\Omega} \mathbb{E}\left[z_{ijt}\right] + \tau_0\mu_0), \tilde{\tau} = \mathbb{E}\left[\tau\right] \sum_{(i,j,t)\in\Omega} o_{ijt} + \tau_0, \tag{15}$$

where $z_{ijt} = y_{ijt} - \phi_i - \theta_j - \eta_t - \sum_{k=1}^r u_{ik}v_{jk}x_{tk}$ and its variational expectation is given by

$$\mathbb{E}\left[z_{ijt}\right] = y_{ijt} - \mathbb{E}\left[\phi_i\right] - \mathbb{E}\left[\theta_j\right] - \mathbb{E}\left[\eta_t\right] - \sum_{k=1}^r \mathbb{E}\left[u_{ik}\right]\mathbb{E}\left[v_{jk}\right]\mathbb{E}\left[x_{tk}\right]. \tag{16}$$

3.3.3. The variational posterior distribution of $\{\boldsymbol{\phi}, \boldsymbol{\theta}, \boldsymbol{\eta}\}$

As can be seen from the Bayesian graphical model in Fig. 3 and the prior setting in Eq. (8), bias vectors $\boldsymbol{\phi}, \boldsymbol{\theta}, \boldsymbol{\eta}$ are expressed by their independent Gaussian elements. Considering the i-th element ϕ_i of $\boldsymbol{\phi} \in \mathbb{R}^m$ as an example, we have

$$\begin{aligned}
\ln q(\phi_i) &= \mathbb{E}_{q(\Theta\backslash\phi_i)}[\ln p(\mathcal{Y}_\Omega, \Theta)] + \text{const} \\
&= -\frac{1}{2}(\mathbb{E}\left[\tau\right] \sum_{j,t:(i,j,t)\in\Omega} o_{ijt} + \tau_0)\phi_i^2 + (\mathbb{E}\left[\tau\right] \sum_{j,t:(i,j,t)\in\Omega} \mathbb{E}\left[f_{ijt}\right] + \tau_0\mu_0)\phi_i + \text{const},
\end{aligned} \tag{17}$$

where $\sum_{j,t:(i,j,t)\in\Omega}$ denotes the sum over $j \in \{1, 2, ..., n\}$ and $t \in \{1, 2, ..., f\}$ with specific i in the index set Ω.

We therefore derive the variational posterior $q(\phi_i) = \mathcal{N}(\tilde{\mu}_\phi, \tilde{\tau}_\phi^{-1})$ with such updates

$$\tilde{\mu}_\phi = \tilde{\tau}_\phi^{-1}(\mathbb{E}\left[\tau\right] \sum_{j,t:(i,j,t)\in\Omega} \mathbb{E}\left[f_{ijt}\right] + \tau_0\mu_0), \tilde{\tau}_\phi = \mathbb{E}\left[\tau\right] \sum_{j,t:(i,j,t)\in\Omega} o_{ijt} + \tau_0, \tag{18}$$

where

$$\mathbb{E}\left[f_{ijt}\right] = y_{ijt} - \mathbb{E}\left[\mu\right] - \mathbb{E}\left[\theta_j\right] - \mathbb{E}\left[\eta_t\right] - \sum_{k=1}^r \mathbb{E}\left[u_{ik}\right]\mathbb{E}\left[v_{jk}\right]\mathbb{E}\left[x_{tk}\right]. \tag{19}$$

Once we have the variational posterior distribution $q(\phi_i)$, we can also derive the variational posterior distributions $q(\theta_j)$ and $q(\eta_t)$ in a similar manner respectively.

3.3.4. The variational posterior distribution of $\{U, V, X\}$

Since factor matrices have multi-variate Gaussian prior over their row vectors, thus, for instance, we can write the variational posterior distribution $q(\boldsymbol{u}_i)$ for updating the factor matrix U as follows

$$\begin{aligned}
\ln q(\boldsymbol{u}_i) =& \mathbb{E}_{q(\Theta\backslash\boldsymbol{u}_i)}[\ln p(\mathcal{Y}_\Omega, \Theta)] + \text{const} \\
=& -\frac{1}{2} \sum_{j,t:(i,j,t)\in\Omega} \mathbb{E}[\tau\left(w_{ijt} - \boldsymbol{u}_i^T(\boldsymbol{v}_j \circledast \boldsymbol{x}_t)\right)^2] - \frac{1}{2}\mathbb{E}[(\boldsymbol{u}_i - \boldsymbol{\mu}_u)^T \Lambda_u (\boldsymbol{u}_i - \boldsymbol{\mu}_u)] + \text{const} \\
=& -\frac{1}{2}\boldsymbol{u}_i^T(\mathbb{E}\left[\tau\right] \sum_{j,t:(i,j,t)\in\Omega} \mathbb{E}\left[(\boldsymbol{v}_j \circledast \boldsymbol{x}_t)(\boldsymbol{v}_j \circledast \boldsymbol{x}_t)^T\right] + \mathbb{E}\left[\Lambda_u\right])\boldsymbol{u}_i \\
&+ \frac{1}{2}\boldsymbol{u}_i^T(\mathbb{E}\left[\tau\right] \sum_{j,t:(i,j,t)\in\Omega} \mathbb{E}\left[\boldsymbol{v}_j \circledast \boldsymbol{x}_t\right]\mathbb{E}\left[w_{ijt}\right] + \mathbb{E}\left[\Lambda_u\right]\mathbb{E}\left[\boldsymbol{\mu}_u\right]) + \text{const},
\end{aligned} \tag{20}$$

where the symbol $\circledast$ represents Hadamard product, and $\boldsymbol{u}_i^T(\boldsymbol{v}_j \circledast \boldsymbol{x}_t) = \sum_{k=1}^r u_{ik}v_{jk}x_{tk}$. For brevity, $\mathbb{E}[w_{ijt}] = y_{ijt} - \mathbb{E}[\phi_i] - \mathbb{E}[\theta_j] - \mathbb{E}[\eta_t]$. We have the variational posterior $q(\boldsymbol{u}_i) = \mathcal{N}(\tilde{\boldsymbol{\mu}}_u, \tilde{\Lambda}_u^{-1})$ whose parameters are given by

$$\begin{aligned}
\tilde{\boldsymbol{\mu}}_u &= \tilde{\Lambda}_u^{-1}(\mathbb{E}\left[\tau\right] \sum_{j,t:(i,j,t)\in\Omega} \mathbb{E}\left[\boldsymbol{v}_j \circledast \boldsymbol{x}_t\right]\mathbb{E}\left[w_{ijt}\right] + \mathbb{E}\left[\Lambda_u\right]\mathbb{E}\left[\boldsymbol{\mu}_u\right]), \\
\tilde{\Lambda}_u &= \mathbb{E}\left[\tau\right] \sum_{j,t:(i,j,t)\in\Omega} \mathbb{E}\left[(\boldsymbol{v}_j \circledast \boldsymbol{x}_t)(\boldsymbol{v}_j \circledast \boldsymbol{x}_t)^T\right] + \mathbb{E}\left[\Lambda_u\right],
\end{aligned} \tag{21}$$

where assuming that the vectors $\{\boldsymbol{v}_j, \boldsymbol{x}_t\}, \forall j, t$ are independent (Zhao et al., 2015a), then

$$\begin{aligned}
\mathbb{E}\left[(\boldsymbol{v}_j \circledast \boldsymbol{x}_t)(\boldsymbol{v}_j \circledast \boldsymbol{x}_t)^T\right] &= \mathbb{E}\left[\boldsymbol{v}_j\boldsymbol{v}_j^T\right] \circledast \mathbb{E}\left[\boldsymbol{x}_t\boldsymbol{x}_t^T\right] \\
&= (\mathbb{E}\left[\boldsymbol{v}_j\right]\mathbb{E}\left[\boldsymbol{v}_j^T\right] + \text{cov}(\boldsymbol{v}_j)) \circledast (\mathbb{E}\left[\boldsymbol{x}_t\right]\mathbb{E}\left[\boldsymbol{x}_t^T\right] + \text{cov}(\boldsymbol{x}_t)),
\end{aligned} \tag{22}$$

here, the notation $\text{cov}(\cdot)$ denotes the covariance matrix of a vector.

In order to update the factor matrices V and X, we can do the same with vectors $\boldsymbol{v}_j, j \in \{1, 2, ..., n\}$ and $\boldsymbol{x}_t, t \in \{1, 2, ..., f\}$ while referring to $\boldsymbol{u}_i, i \in \{1, 2, ..., m\}$.

166 *3.3.5. The variational posterior distribution of $\{(\boldsymbol{\mu}_u, \Lambda_u), (\boldsymbol{\mu}_v, \Lambda_v), (\boldsymbol{\mu}_x, \Lambda_x)\}$*

167 According to Eq. (12), by taking derivative of Eq. (13) with respect to $(\boldsymbol{\mu}_u, \Lambda_u)$, the variational posterior
168 $q(\boldsymbol{\mu}_u, \Lambda_u)$ can be analytically derived as

$$
\begin{aligned}
\ln q(\boldsymbol{\mu}_u, \Lambda_u) =& \mathbb{E}_{q(\Theta \backslash \boldsymbol{\mu_u}, \Lambda_u)}[\ln p(\mathcal{Y}_\Omega, \Theta)] + \text{const} \\
=& \frac{1}{2} \ln |\Lambda_u| - \frac{1}{2} (\boldsymbol{\mu}_u - \frac{m\bar{\boldsymbol{u}} + \beta_0 \boldsymbol{\mu}_0}{m + \beta_0})^T [(m + \beta_0) \Lambda_u] (\boldsymbol{\mu}_u - \frac{m\bar{\boldsymbol{u}} + \beta_0 \boldsymbol{\mu}_0}{m + \beta_0}) \\
& + \frac{1}{2}(m + \nu_0 - r - 1) \ln |\Lambda_u| \\
& - \frac{1}{2} \text{tr}((W_0^{-1} + \sum_{i=1}^m (\mathbb{E}[\boldsymbol{u}_i] - \bar{\boldsymbol{u}})(\mathbb{E}[\boldsymbol{u}_i] - \bar{\boldsymbol{u}})^T + \frac{m\beta_0}{m + \beta_0}(\bar{\boldsymbol{u}} - \boldsymbol{\mu}_0)(\bar{\boldsymbol{u}} - \boldsymbol{\mu}_0)^T)\Lambda_u) + \text{const},
\end{aligned}
\tag{23}
$$

169 recall that there is a Gaussian-Wishart prior placing on the hyper-parameters $(\boldsymbol{\mu}_u, \Lambda_u)$ as described in Eq. (8),
170 we therefore have the variational posterior $q(\boldsymbol{\mu}_u, \Lambda_u) = \mathcal{N}(\boldsymbol{\mu}_u \mid \tilde{\boldsymbol{\mu}}_u^*, (\tilde{\beta}_u^* \Lambda_u)^{-1}) \mathcal{W}(\Lambda_u \mid \tilde{W}_u^*, \tilde{\nu}_u^*)$ as follows

$$
\begin{aligned}
\tilde{\boldsymbol{\mu}}_u^* &= \frac{m\bar{\boldsymbol{u}} + \beta_0 \boldsymbol{\mu}_0}{m + \beta_0}, \tilde{\beta}_u^* = \beta_0 + m, \tilde{\nu}_u^* = \nu_0 + m, \\
(\tilde{W}_u^*)^{-1} &= W_0^{-1} + \sum_{i=1}^m (\mathbb{E}[\boldsymbol{u}_i] - \bar{\boldsymbol{u}})(\mathbb{E}[\boldsymbol{u}_i] - \bar{\boldsymbol{u}})^T + \frac{m\beta_0}{m + \beta_0}(\bar{\boldsymbol{u}} - \boldsymbol{\mu}_0)(\bar{\boldsymbol{u}} - \boldsymbol{\mu}_0)^T,
\end{aligned}
\tag{24}
$$

171 where $\bar{\boldsymbol{u}} = \frac{1}{m}\sum_{i=1}^m \mathbb{E}[\boldsymbol{u}_i]$.
172 In such case, the Eqs. (23) and (24) can help us to derive the variational posterior of $(\boldsymbol{\mu}_v, \Lambda_v)$ and $(\boldsymbol{\mu}_x, \Lambda_x)$.

173 *3.3.6. The variational posterior distribution of τ*

174 Consider the precision term $\tau \in \mathbb{R}$ which controls all tensor elements, we write its variational posterior referring
175 to the above derivations as

$$
\begin{aligned}
\ln q(\tau) =& \mathbb{E}_{q(\Theta \backslash \tau)}[\ln p(\mathcal{Y}_\Omega, \Theta)] + \text{const} \\
=& (a_0 + \frac{1}{2}\sum_{(i,j,t) \in \Omega} o_{ijk} - 1) \ln \tau - (b_0 + \frac{1}{2}\sum_{(i,j,t) \in \Omega} \mathbb{E}[(y_{ijt} - g_{ijt})^2])\tau + \text{const},
\end{aligned}
\tag{25}
$$

176 and it is straightforward to have the variational posterior $q(\tau) = \text{Gamma}(\tilde{a}_\tau, \tilde{b}_\tau)$ as follows

$$
\begin{aligned}
\tilde{a}_\tau &= a_0 + \frac{1}{2}\sum_{(i,j,t) \in \Omega} o_{ijk}, \\
\tilde{b}_\tau &= b_0 + \frac{1}{2}\sum_{(i,j,t) \in \Omega} \mathbb{E}[(y_{ijt} - g_{ijt})^2],
\end{aligned}
\tag{26}
$$

177 where we define $g_{ijt} = \mu + \phi_i + \theta_j + \eta_t + \sum_{k=1}^r u_{ik} v_{jk} x_{tk}$.

178 *3.3.7. Lower bound of model evidence*

179 The lower bound plays an essential role in the VB derivations. If in some cases we want to maximize the
180 marginal probability, we can instead maximize its lower bound. As a result, when using VB to implement a tensor
181 factorization model, we can check the value of lower bound to determine the convergence of the algorithm because
182 $\mathcal{L}(q)$ at each epoch should increase sequentially. To be specific, the lower bound regarding Eq. (10) is given by

$$
\begin{aligned}
\mathcal{L}(q) =& \mathbb{E}_{q(\Theta)}[\ln p(\mathcal{Y}_\Omega, \Theta)] + H(q(\Theta)) \\
=& \mathbb{E}_q[\ln p(\mathcal{Y}_\Omega \mid \Theta)] + \mathbb{E}_q[\ln p(\mu)] + \mathbb{E}_q[\ln p(\boldsymbol{\phi})] + \mathbb{E}_q[\ln p(\boldsymbol{\theta})] + \mathbb{E}_q[\ln p(\boldsymbol{\eta})] \\
& + \mathbb{E}_q[\ln p(U \mid \boldsymbol{\mu}_u, \Lambda_u)] + \mathbb{E}_q[\ln p(V \mid \boldsymbol{\mu}_v, \Lambda_v)] + \mathbb{E}_q[\ln p(X \mid \boldsymbol{\mu}_x, \Lambda_x)] \\
& + \mathbb{E}_q[\ln p(\boldsymbol{\mu}_u, \Lambda_u)] + \mathbb{E}_q[\ln p(\boldsymbol{\mu}_v, \Lambda_v)] + \mathbb{E}_q[\ln p(\boldsymbol{\mu}_x, \Lambda_x)] + \mathbb{E}_q[\ln p(\tau)] \\
& - \mathbb{E}_q[\ln q(\mu)] - \mathbb{E}_q[\ln q(\boldsymbol{\phi})] - \mathbb{E}_q[\ln q(\boldsymbol{\theta})] - \mathbb{E}_q[\ln q(\boldsymbol{\eta})] \\
& - \mathbb{E}_q[\ln q(U)] - \mathbb{E}_q[\ln q(V)] - \mathbb{E}_q[\ln q(X)] \\
& - \mathbb{E}_q[\ln q(\boldsymbol{\mu}_u, \Lambda_u)] - \mathbb{E}_q[\ln q(\boldsymbol{\mu}_v, \Lambda_v)] - \mathbb{E}_q[\ln q(\boldsymbol{\mu}_x, \Lambda_x)] - \mathbb{E}_q[\ln q(\tau)],
\end{aligned}
\tag{27}
$$

183 where all expectations are with respect to the posterior distribution q. The first term is an expectation of the
184 joint distribution. The second to the eighth terms are the expectations of log-priors over the global parameter,
185 bias vectors, and factor matrices. The ninth to the eleventh terms denote the expectations of log-priors over
186 hyper-parameters. The twelfth term is the expectation of log-prior over τ. In addition, the last 11 terms are
187 entropy of the posterior distribution q over Θ.

3.4. Implementing BATF

In above, since our posterior inference based tensor factorization is inferred in a VB framework, the question is how to learn our interested parameters $\{\mu, \phi, \theta, \eta, U, V, X\}$ (i.e., global parameter, bias vectors, and factor matrices) from the partially observed tensor $\mathcal{Y}_\Omega$. The feasible solution is by updating the model parameters and hyper-parameters (see Fig. 3) alternatively. We can trace back to the above derivations and see more details about it from Algorithm 1.

Algorithm 1 Bayesian augmented tensor factorization (BATF)

Input: incomplete data tensor $\mathcal{Y}_\Omega \in \mathbb{R}^{m \times n \times f}$, indicator tensor $\mathcal{O} \in \mathbb{R}^{m \times n \times f}$, global parameter μ, bias vectors $\{\phi, \theta, \eta\}$ and factor matrices $\{U, V, X\}$.

Output: estimated tensor $\hat{\mathcal{Y}} \in \mathbb{R}^{m \times n \times f}$, and updated μ, $\{\phi, \theta, \eta\}$ and $\{U, V, X\}$.

    Initialize $\tau, a_0, b_0, \beta_0 = 1$, $\mu_0 = 0, \tau_0 = 1$, $\nu_0 = r$, $\boldsymbol{\mu}_0 = \mathbf{0}$, and $W_0 = I$ (identity matrix).

1: **repeat**
2:     Update the posterior of global parameter $q(\mu)$ using Eq. (15).
3:     Update the posterior of hyper-parameters $q(\boldsymbol{\mu}_u, \Lambda_u)$, $q(\boldsymbol{\mu}_v, \Lambda_v)$ and $q(\boldsymbol{\mu}_x, \Lambda_x)$ using Eq. (24) and its similar inference results.
4:     **for** $i = 1$ to m **do**
5:         Update the posterior of bias $q(\phi_i)$ using Eq. (18).
6:         Update the posterior of factor $q(\boldsymbol{u}_i)$ using Eq. (21).
7:     **end for**
8:     **for** $j = 1$ to n **do**
9:         Update the posterior of bias $q(\theta_j)$ similar to Eq. (18).
10:        Update the posterior of factor $q(\boldsymbol{v}_j)$ similar to Eq. (21).
11:     **end for**
12:     **for** $t = 1$ to f **do**
13:        Update the posterior of bias $q(\eta_t)$ similar to Eq. (18).
14:        Update the posterior of factor $q(\boldsymbol{x}_t)$ similar to Eq. (21).
15:     **end for**
16:     Update the posterior of precision $q(\tau)$ using Eq. (26).
17:     Evaluate the lower bound $\mathcal{L}(q)$ using Eq. (27).
18: **until** convergence.

---

4. Experiments

In this section, our goal is to learn an expressive representation of urban traffic state that is semantically meaningful, so that we can identify both explicit patterns and latent factors. To this end, we carry out a wide range of empirical examinations to broadly investigate the performance of BATF. Relying on the urban traffic speed data set, we first evaluate how well BATF works for tensor completion compared to the baseline models. We then survey the learned latent factors as well as the explicit patterns, and further show the semantic interpretations of each one and their combination. Finally, we demonstrate the robustness of BATF in the missing data imputation task under different missing scenarios with varying missing rates.

4.1. Details of experiment setting

Data set. We utilize a publicly available traffic speed data set (see https://doi.org/10.5281/zenodo.1205229) which is evaluated in the recent papers (Chen et al., 2018, 2019). This data set is collected from 214 road segments in Guangzhou, China within two months (i.e., 61 days from August 1, 2016 to September 30, 2016) at 10-minute interval (144 time intervals per day). The speed data can be organized as a third-order tensor (road segment $\times$ day $\times$ time interval, with a size of $214 \times 61 \times 144$). There are about 1.29% missing values in the raw data set.

Experiment setup. The main task of this work is missing data imputation, therefore, we first follow two missing data scenarios, including random missing and non-random (fiber) missing. Then, we set our tensor completion task with 10%, 30%, and 50% missing rates under both two scenarios. When training BATF model, we use rank $r = 80$ in the case of random missing. In order to prevent overfitting, we consider rank $r = 20, 15, 10$ for BATF model at 10%, 30%, and 50% non-random missing rates, respectively. The maximum epoch for BATF model is set to 200. The Matlab code for implementing BATF is available at https://github.com/sysuits/BATF.

Performance metrics. The mean absolute percentage error (MAPE) and root mean square error (RMSE) are used to evaluate the model performance, i.e.,

$$\text{MAPE} = \frac{1}{N} \sum_{i=1}^{N} \frac{|y_i - \hat{y}_i|}{y_i}, \text{RMSE} = \sqrt{\frac{1}{N} \sum_{i=1}^{N} (y_i - \hat{y}_i)^2}, \tag{28}$$

where N is the total number of missing values, and y_i and $\hat{y}_i$ are the actual value of a missing element and its imputation, respectively.

Baselines. We consider two fully Bayesian tensor factorization models, the Bayesian CP factorization (BCPF, Zhao et al. (2015a)) and the Bayesian Gaussian CP decomposition (BGCP, Chen et al. (2019)), as evaluation baselines. BCPF and BGCP are implemented by VB and MCMC, respectively.

4.2. Performance of missing data imputation

With the above settings, we compare the proposed BATF model to three state-of-the-art models, including BCPF (Zhao et al., 2015b), BGCP (Chen et al., 2019), and STD (Chen et al., 2018). Table 1 shows the imputation performance of these models where BATF, BCPF, and BGCP share the same rank r. Note that the comparison between BGCP and other models (e.g., daily average, kNN, and HaLRTC) was demonstrated at the work of Chen et al. (2019). In this study, we only investigate the imputation performance of tensor based models.

Our first experiment examines the performance of different models in the random missing scenario. One can easily find that the Bayesian tensor factorization models have significant improvement over STD and are less sensitive to the increasing missing rate. Thus, it also supports that Bayesian inference methods for tensor factorization are effective for dealing with the sparsity issue (Zhao et al., 2015a). Thanks to the flexible conjugate prior setting, BATF and BGCP get slightly better results than BCPF as they have more parameters to fit the data. However, when the tensor behaves with an increasing amount of missing values, these models accordingly exhibit growing errors.

In the second experiment, we present imputation performance in the non-random missing scenario, which is a more realistic temporally correlated scenario following Chen et al. (2018). Since Bayesian tensor factorization models are sensitive to the rank parameter, we choose the rank r as 20, 15, and 10 for the missing rate of 10%, 30%, and 50%, respectively. From the comparison, we see that our BATF performs better than the other two models, which shows the structural benefit of augmented tensor factorization. The results of Table 1 also suggest that the presentation learned by BATF is significantly more capable of imputing missing data than other competing models, and BATF's results are also less sensitive to the increasing missing rate.

Due to the temporally correlated corruption in the non-random missing scenario, it becomes difficult to utilize the algebraic structure and collaborative information. Comparing to the random missing scenario, we can find that the errors at the non-random missing scenario are relatively higher. Even with the same missing rate, the non-random missing scenario is more difficult to tackle than the random missing. In practice, we can see that BCPF fails to work in the non-random missing scenario with the given ranks (see Table 1).

Table 1: MAPE/RMSE scores of tensor completion models for the urban traffic speed data set.

	Random missing			Non-random missing		
	10% ($r = 80$)	30% ($r = 80$)	50% ($r = 80$)	10% ($r = 20$)	30% ($r = 15$)	50% ($r = 10$)
BATF	0.0825/3.5745	0.0834/3.5969	0.0841/3.6290	0.0976/4.1252	0.0995/4.2256	0.1029/4.3557
BCPF	0.0832/3.5988	0.0843/3.6340	0.0852/3.6784	-	-	-
BGCP	0.0823/3.5614	0.0827/3.5775	0.0833/3.6009	0.0980/4.1413	0.0999/4.2425	0.1048/4.4419
STD	0.0888/3.7708	0.0936/3.9286	0.0993/4.1253	0.1019/4.1881	0.1068/4.4029	0.1133/4.6291

## 4.3. Semantic interpretations of BATF

In this study, we are interested in BATF having not only the imputation power but also the ability to discover interpretable patterns. To provide more insights into the effectiveness of BATF, we start by summarizing the explicit patterns of BATF (see Fig. 4) and explore the semantic interpretations of BATF. Fig. 4(a) presents the curves of global parameters of BATF by running 30 times. It is intuitive that the average of 30 global parameter curves is extremely close to the actual mean of observations (i.e., 39.01 km/h). This experimentally illustrates that the global parameter controlling all tensor elements is used to capture the mean standard of partially observed data.

Fig. 4(b) and Fig. 4(c) show the bias values corresponding to 214 road segments and 144 time intervals respectively. From Fig. 4(b), there are about half of road segments obtaining biases above 0 and up to 20 km/h, while others between -15 km/h and 0 km/h. The bias value also has its real-world meanings. For example, if one road segment has a relatively high (positive) bias, we can generally say that the traffic state of this road segment is better than the normal standard of the whole network. The bias of one road segment is indeed a relative value over the global average.

Fig. 4(c) illustrates that negative biases appear in daytime, while positive biases appear in night. Specifically, the bias reaches its lowest during the evening peak hours, and the bias is relatively higher in the morning peak hours. Fig. 4(d) shows the heatmap of summed biases over day and time interval dimensions. It enables us to
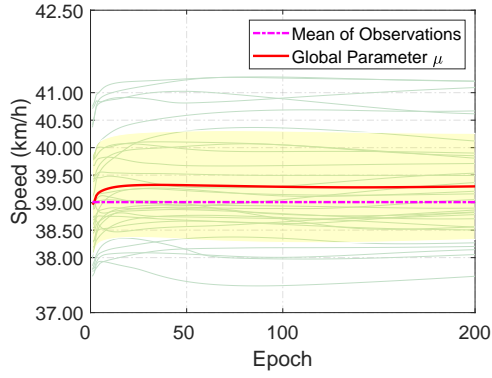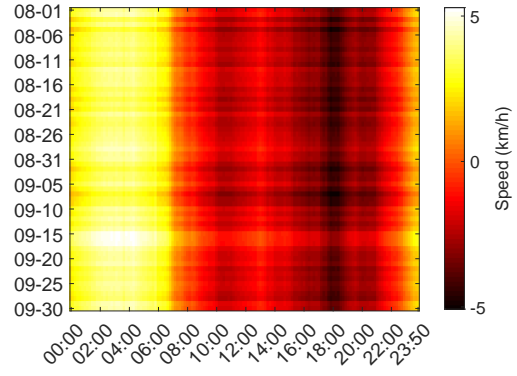
(a) Global parameter at each epoch.
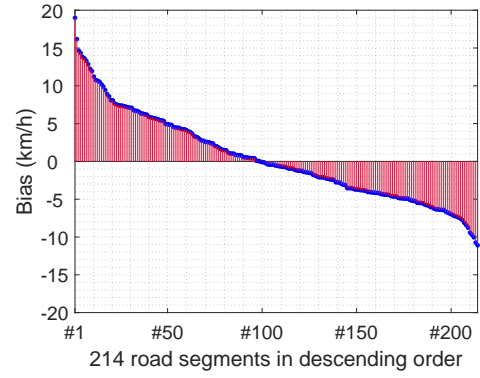
(b) Biases of 214 road segments.
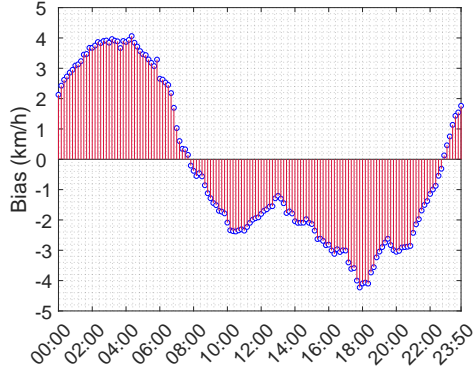
(c) Biases of 144 time intervals.

(d) Summed biases over day and time interval dimensions.

Figure 4: The explicit patterns (i.e., global parameter and biases) of BATF at the 50% non-random missing rate with $r = 10$.

understand the time-evolving traffic patterns across two dimension simultaneously. Note that all these findings are also consistent with the daily trend of traffic state reported by Chen et al. (2018).

To reinforce our interpretation that these explicit patterns are semantically meaningful, in Fig. 5, we present an example which covers the time series of actual values versus the one of its imputation of road segment #1. The simple combination of explicit patterns (i.e., global parameter and biases) provides rough trends of traffic states. By further putting explicit patterns and latent factors together, we can find that the estimated time series using BATF is closer to the actual one. Thus, in terms of explicit patterns, our newly formulated Eq. (4) has more semantically meaningful representations than the conventional tensor factorization models (see Eq. (1)).

Regarding the failure of BCPF in the non-random missing scenario (see Table 1), we choose the experiment for BCPF at the 30% missing rate with its rank being $r = 5, 10$. Fig. 6 presents the RMSE and lower bound value of BCPF for investigating the train-test performance. In Table 1, it is worth noting that BCPF cannot work when setting the same rank r to BATF and BGCP models. However, observing Fig. 6(b), even placing a smaller rank, BCPF still suffers from the overfitting problem.
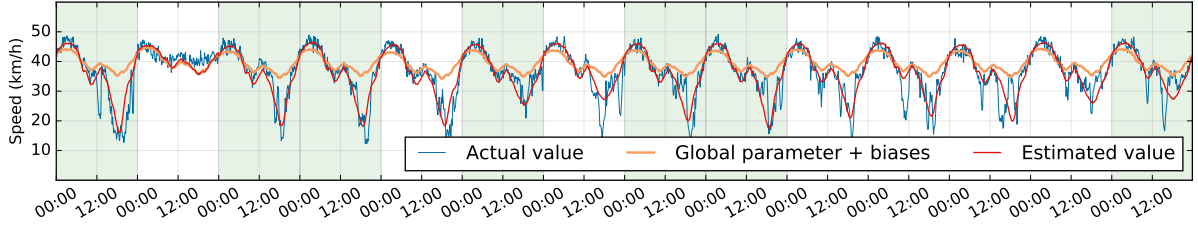
(a) Time series of actual and estimated speed within two weeks from August 1 to 14.
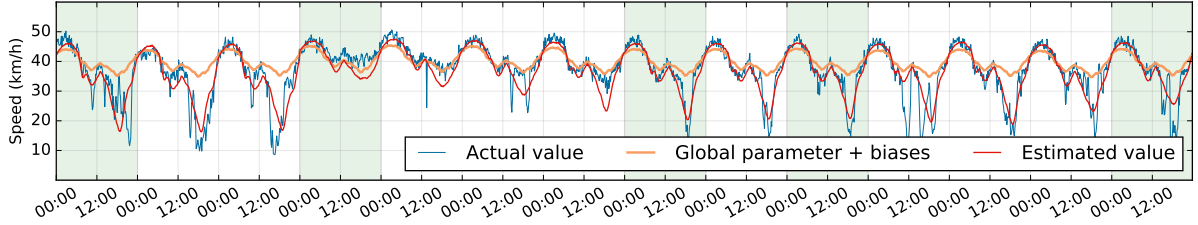
(b) Time series of actual and estimated speed within two weeks from September 12 to 25.

Figure 5: The imputation performance of BATF at the 50% non-random missing rate with $r = 10$, where the estimated result of road segment #1 is selected as an example. In the both two panels, white rectangles represent fiber missing (i.e., speed observations are lost in a whole day), and green rectangles indicate partially observed data.
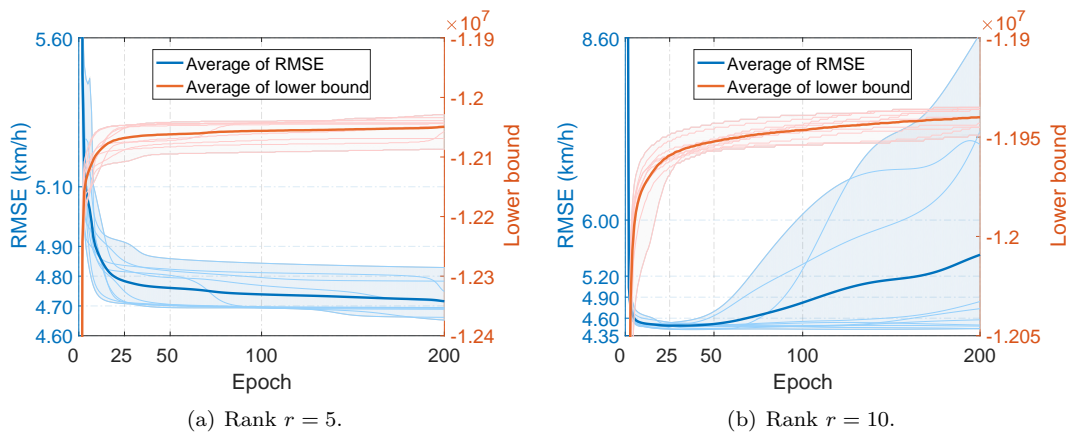

(a) Rank $r = 5$.

(b) Rank $r = 10$.

Figure 6: RMSEs and lower bound values of BCPF model ran 10 times at the 30% missing rate.

5. Conclusion

In this study, we propose an augmented tensor factorization with fully Bayesian treatment to impute the missing traffic data accurately. First, the factorization based on Bayesian inference is less sensitive to the data sparsity where the results reported by Bayesian tensor factorization models are in effect more tolerant to the increasing missing rate (see Table 1). Then, from the empirical studies, when setting the non-random missing

rate ranging from 10% to 50%, we demonstrated that BATF performs best among its competing models. At the random missing scenario, BATF also achieves competitive imputation results.

Finally, as our experiments demonstrated, competing tensor factorization models failed to capture explicit patterns and their application scenario is limited because of our complex data and the overfitting issue. Instead, the proposed BATF achieves generalization performance of Bayesian tensor factorization and combines explicit patterns and latent factors together. Our formula (see Eq. (4)) incorporating generic forms of domain knowledge also provide more insights into the effectiveness of tensor factorization.

Acknowledgement

References

Asif, M. T., Mitrovic, N., Dauwels, J., Jaillet, P., 2016. Matrix and tensor based methods for missing data estimation in large traffic networks. IEEE Transactions on Intelligent Transportation Systems 17 (7), 1816–1825.

Chen, X., He, Z., Sun, L., 2019. A bayesian tensor decomposition approach for spatiotemporal traffic data imputation. Transportation Research Part C: Emerging Technologies 98, 73 – 84.
URL http://www.sciencedirect.com/science/article/pii/S0968090X1830799X

Chen, X., He, Z., Wang, J., 2018. Spatial-temporal traffic speed patterns discovery and incomplete data recovery via svd-combined tensor decomposition. Transportation Research Part C: Emerging Technologies 86, 59–77.

Hu, C., Rai, P., Chen, C., Harding, M., Carin, L., 2015. Scalable bayesian non-negative tensor factorization for massive count data. In: Proceedings, Part II, of the European Conference on Machine Learning and Knowledge Discovery in Databases - Volume 9285. ECML PKDD 2015. Springer-Verlag New York, Inc., New York, NY, USA, pp. 53–70.
URL http://dx.doi.org/10.1007/978-3-319-23525-7_4

Kolda, T. G., Bader, B. W., 2009. Tensor decompositions and applications. SIAM Reviw 51 (3), 455–500.

Koren, Y., Bell, R., Volinsky, C., Aug 2009. Matrix factorization techniques for recommender systems. Computer 42 (8), 30–37.

Laa, I., Olabarrieta, I. I., Vlez, M., Ser, J. D., 2018. On the imputation of missing data for road traffic forecasting: New insights and novel techniques. Transportation Research Part C: Emerging Technologies 90, 18 – 33.
URL http://www.sciencedirect.com/science/article/pii/S0968090X18302535

Li, L., Li, Y., Li, Z., 2013. Efficient missing data imputing for traffic flow by considering temporal and spatial dependence. Transportation research part C: emerging technologies 34, 108–120.
URL http://dx.doi.org/10.1016/j.trc.2013.05.008

Liu, J., Musialski, P., Wonka, P., Ye, J., 2013. Tensor completion for estimating missing values in visual data. IEEE Transactions on Pattern Analysis and Machine Intelligence 35 (1), 208–220.

Qu, L., Li, L., Zhang, Y., Hu, J., 2009. Ppca-based missing data imputation for traffic flow volume: A systematical approach. IEEE Transactions on Intelligent Transportation Systems 10 (3), 512–522.

Qu, L., Zhang, Y., Hu, J., Jia, L., Li, L., June 2008. A bpca based missing value imputing method for traffic flow volume data. In: 2008 IEEE Intelligent Vehicles Symposium. pp. 985–990.

Rai, P., Hu, C., Harding, M., Carin, L., 2015. Scalable probabilistic tensor factorization for binary and count data. In: Proceedings of the 24th International Conference on Artificial Intelligence. IJCAI'15. AAAI Press, pp. 3770–3776.
URL http://dl.acm.org/citation.cfm?id=2832747.2832775

Rai, P., Wang, Y., Guo, S., Chen, G., Dunson, D., Carin, L., 2014. Scalable bayesian low-rank decomposition of incomplete multiway tensors. In: Xing, E. P., Jebara, T. (Eds.), Proceedings of the 31st International Conference on Machine Learning. Vol. 32 of Proceedings of Machine Learning Research. PMLR, Bejing, China, pp. 1800–1808.
URL http://proceedings.mlr.press/v32/rai14.html

Ran, B., Tan, H., Wu, Y., Jin, P. J., 2016. Tensor based missing traffic data completion with spatial-temporal correlation. Physica A: Statistical Mechanics and its Applications 446, 54–63.

Rodrigues, F., Henrickson, K., Pereira, F. C., 2018. Multi-output gaussian processes for crowdsourced traffic data imputation. IEEE Transactions on Intelligent Transportation Systems, 1–10.

Salakhutdinov, R., Mnih, A., 2008. Bayesian probabilistic matrix factorization using markov chain monte carlo. In: Proceedings of the 25th International Conference on Machine Learning. ICML '08. ACM, New York, NY, USA, pp. 880–887.
    URL http://doi.acm.org/10.1145/1390156.1390267

Schein, A., Zhou, M., Blei, D., Wallach, H., 20–22 Jun 2016. Bayesian poisson tucker decomposition for learning the structure of international relations. In: Balcan, M. F., Weinberger, K. Q. (Eds.), Proceedings of The 33rd International Conference on Machine Learning. Vol. 48 of Proceedings of Machine Learning Research. PMLR, New York, New York, USA, pp. 2810–2819.
    URL http://proceedings.mlr.press/v48/schein16.html

Tan, H., Feng, G., Feng, J., Wang, W., Zhang, Y.-J., Li, F., 2013a. A tensor-based method for missing traffic data completion. Transportation Research Part C: Emerging Technologies 28, 15 – 27, euro Transportation: selected paper from the EWGT Meeting, Padova, September 2009.
    URL http://www.sciencedirect.com/science/article/pii/S0968090X12001532

Tan, H., Yang, Z., Feng, G., Wang, W., Ran, B., 2013b. Correlation analysis for tensor-based traffic data imputation method. Procedia-Social and Behavioral Sciences 96, 2611–2620.

Xiong, L., Chen, X., Huang, T.-K., Schneider, J., Carbonell, J. G., 2010. Temporal collaborative filtering with bayesian probabilistic tensor factorization. In: Proceedings of the 2010 SIAM International Conference on Data Mining. SIAM, pp. 211–222.
    URL http://epubs.siam.org/doi/abs/10.1137/1.9781611972801.19

Zhao, Q., Zhang, L., Cichocki, A., 2015a. Bayesian cp factorization of incomplete tensors with automatic rank determination. IEEE Transactions on Pattern Analysis and Machine Intelligence 37 (9), 1751–1763.

Zhao, Q., Zhang, L., Cichocki, A., 2015b. Bayesian sparse tucker models for dimension reduction and tensor completion. CoRR abs/1505.02343.
    URL http://arxiv.org/abs/1505.02343